

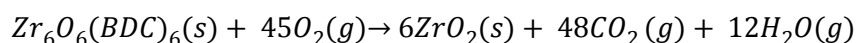
## Supporting Informations

***On the importance of combining bulk- and surface-active sites to maximize the catalytic activity of metal-organic frameworks for the oxidative dehydrogenation of alcohols using alkyl hydroperoxides as hydride acceptors***

P. Gairola, F. Averseng, Y. Millot, J-M. Krafft, F. Launay, P. Massiani, C. Jolival, J. Reboul\*

### Comment S1. Calculation of missing linker defects using TGA analysis

The complete decomposition of ideal dehydroxylated UiO-66 is shown in the equation below:



The complete dehydroxylated UiO-66 with molecular formula  $\text{Zr}_6\text{O}_6(\text{BDC})_6$  has a molecular weight 2.2 factor higher than  $6\text{ZrO}_2$ , the only solid end product of the UiO-66 decomposition. If the solid end product is normalized to 100%, then the plateau observed for temperatures comprised between  $350^\circ\text{C}$  and  $450^\circ\text{C}$ , which represents the completely dehydroxylated material corresponds to 220% in the case of undefective UiO-66 (noted  $W_{\text{ideal plateau}}$  plateau in the figure). The number of defects in the UiO-66 synthesized in this study is deduced from the difference between the wt% value at which this plateau is observed experimentally (noted  $W_{\text{experimental plateau}}$  in the following figure) and  $W_{\text{ideal plateau}}$ .<sup>1</sup>

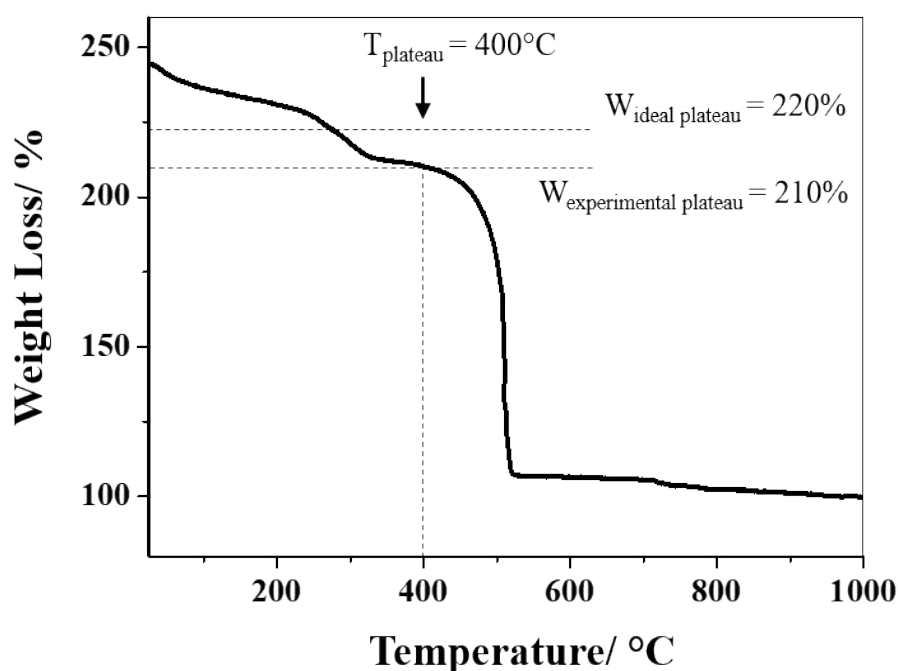
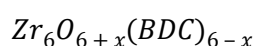


Figure: TGA of UiO-2-1.

The formula of complete dehydroxylated defective UiO-66 is:



Where x corresponds to number of missing linkers per unit formula.

The weight contribution per BDC linker in the case of ideal UiO-66 can be derived by taking the difference between the ideal TGA plateau i.e. 220% and weight of solid end product which is 100%

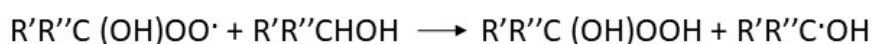
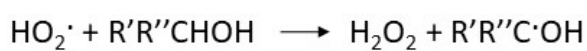
divided by 6 (ideal number of organic linker). It is equal to 20.03%. Then the number of missing linkers x is equal to:

$$6 - x = \frac{W_{\text{experimental plateau}} - 100\%}{20.03\%}$$

$$6 - x = \frac{210\% - 100\%}{20.03\%} = 5.5$$

**Comment S2.** Two possible mechanisms were proposed for the oxidation of alcohols in the presence of hydroperoxyl radicals. The first mechanism requires the occurrence of dissolved O<sub>2</sub> within the medium while the second mechanism does not. Carbonyl products are red framed. Various radical species can be formed during these reactions. None of them was detected by ESR analysis in the presence of DMPO.

First possible alcohol oxidation route:



Second possible oxidation route:



**Table S1.** Comparison of the performances of the UiO-66 synthesized in this work with MOF-based catalysts devoted to benzyl alcohol oxidation with *tert-butyl hydroperoxide* as oxidant reported in the literature.

ref	Material	T (°C)	TBHP/alcohol (molar ratio)	MOF/alcohol (mg/mmol)	Benzaldehy de Yield (%)	Alcohol conversion (%)	Selectivity (%)	Time (h)	Notes
2	Cu-MOF	40	2.26	20	69	76	91	6	Catalysis in CH <sub>2</sub> Cl <sub>2</sub> as solvent
3	Co-MOF	90	2	3.4	89		87	1.5	Degraded after 3 cycles,
4	UoB-2 (Ni-MOF)	65	2	22.5	95	98	97	1	Activity decreases after 4 runs
5	Fe-MOF-808	90	2	102.7	95	99	96	9	Need a Fe-grafting step
6	FePorphyrin-HKUST	25	2.5	34	-	28	-	48	Need to incorporate FePorphyrin active sites
7	Co-MOF	70	1.5	47.5	-	77	-	20	MOF made of expensive linkers
8	Fe <sub>3</sub> O <sub>4</sub> @MIL-101a	70	4	40	43	44	98	12	Need to incorporate Fe <sub>3</sub> O <sub>4</sub> active species within pore
<i>This work</i>	<b>UiO-66</b>	<b>40</b>	<b>2 or 1</b>	<b>120</b>	<b>89</b>	<b>95</b>	<b>93</b>	<b>5</b>	<b>-No post-synthesis modification steps.</b> <b>-No incorporation of active species.</b> <b>-Cheap ligands</b>

**Table S2.** MOF-based catalysts devoted to benzyl alcohol oxidation with *molecular oxygen* as oxidant reported in the literature.

ref	Material	T (°C)	O <sub>2</sub> pressure (bar)	MOF/alcohol (mg/mmol)	Benzaldehyde Yield (%)	Alcohol conversion (%)	Selectivity (%)	Time (h)	Notes
9	Au/MIL-101(Cr)	80	1.01	410	98	99	99	1	- Incorporation of gold nanoparticles within the MOF -Use of expensive gold precursors
10	Au/MOF-5	80	5	99	0 (91% in the ester PhCO <sub>2</sub> Me)	99	0 (for aldehyde)	3	- Incorporation of gold nanoparticles within the MOF -use of expensive gold precursors -Requires the addition of a base (K <sub>2</sub> CO <sub>3</sub> )
11	Au/UiO-66	80	1.01	0.52 High Au loading (= 8 wt %)	53.7	53.8	-	10	- Incorporation of gold nanoparticles within the MOF -Use of expensive gold precursors -Requires the addition of a base (K <sub>2</sub> CO <sub>3</sub> )
12	Cu <sub>3</sub> (BTC) <sub>2</sub> (HKUST-1)	75	1.01	150	89	-	-	22	-Use of TEMPO -Requires the addition of a base (Na <sub>2</sub> CO <sub>3</sub> )

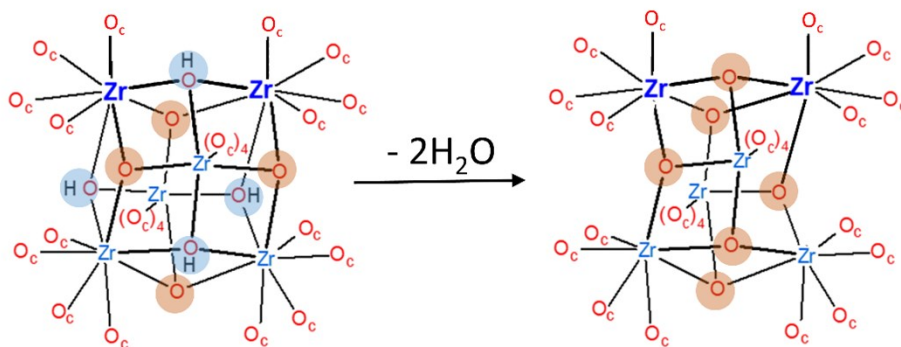


**Figure S1.** Dehydroxylation of the  $Zr_6$  units under treatment at 300°C.

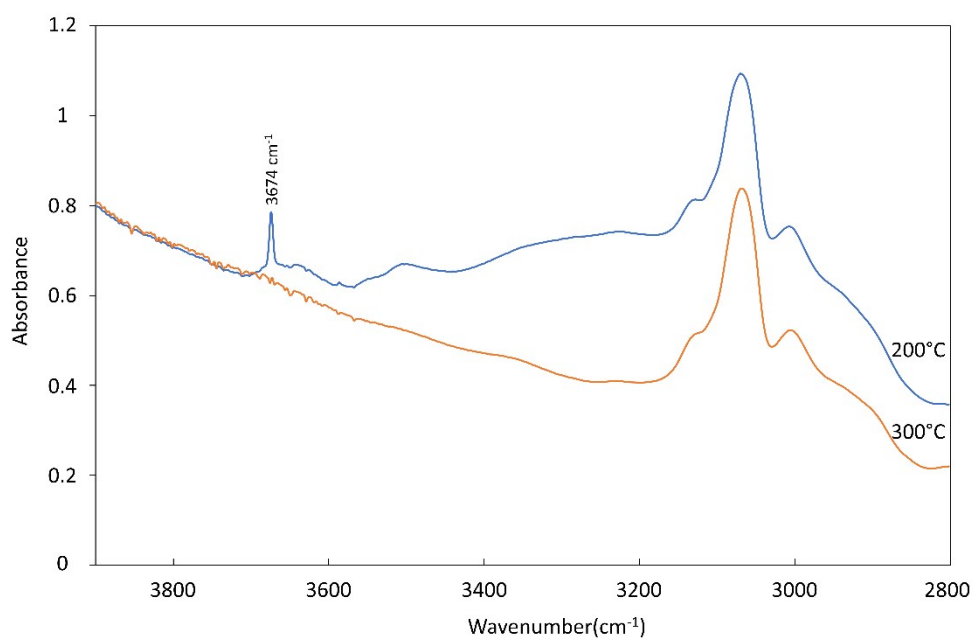


**Figure S2.** FT-IR spectra of UiO-1-9 treated at 200°C (blue line) and at 300°C (red line) collected under the same conditions as those used to perform the IR spectroscopy of CO adsorbed on the same sample (Figure 4Ba in the main manuscript).

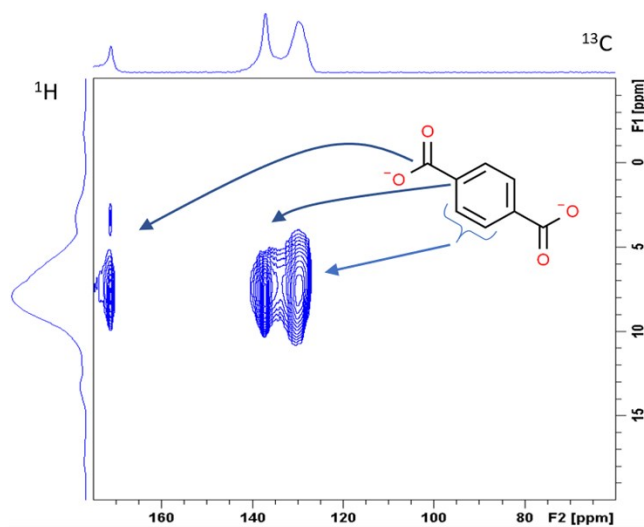


**Figure S3.** H-C cross coupling (a) and Het Core experiment.

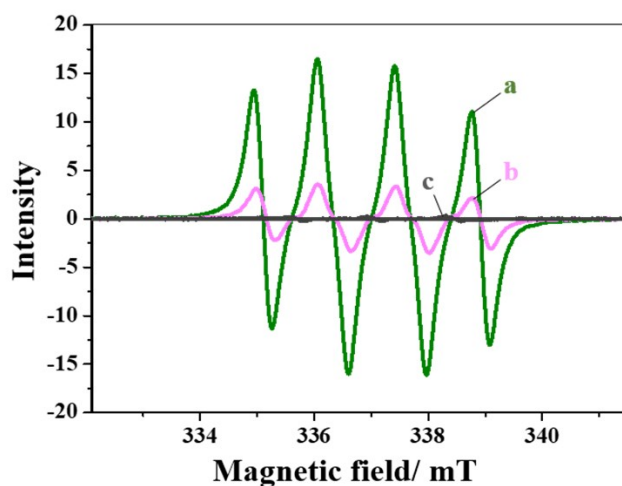


**Figure S4.** Electron spin resonance (ESR) analyses at liquid nitrogen temperature of (a) the TBHP batch mixed with an acetonitrile solution of DMPO as spin trap, (b) the same solution after the addition of benzyl alcohol, and (c) the benzyl alcohol oxidation solution when adding the DMPO after 5 h of reaction.

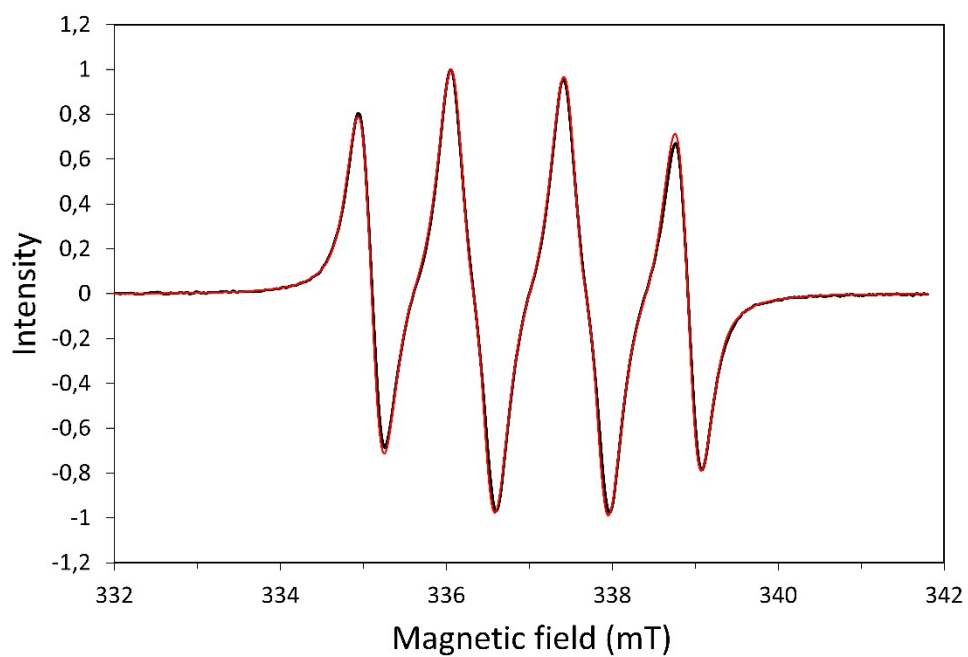


**Figure S5.** Simulated electron spin resonance (ESR) spectrum of the DMPO-OOH adduct (red line) and ESR spectrum achieved at 77K obtained after analyzing the TBHP batch mixed with an acetonitrile solution of DMPO (black line).

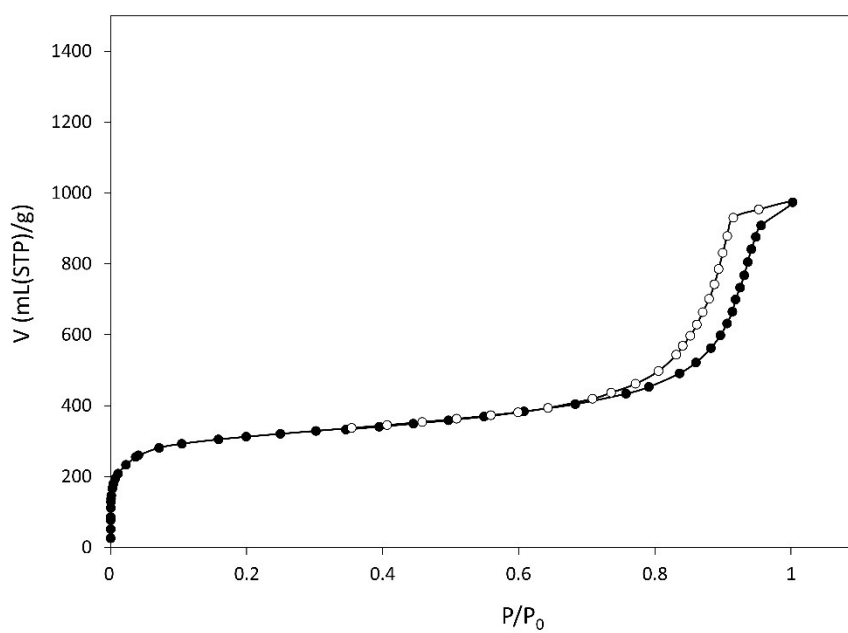


**Figure S6.** N<sub>2</sub> adsorption and desorption isotherms measured at 77K with the sample UiO-0.5-9.



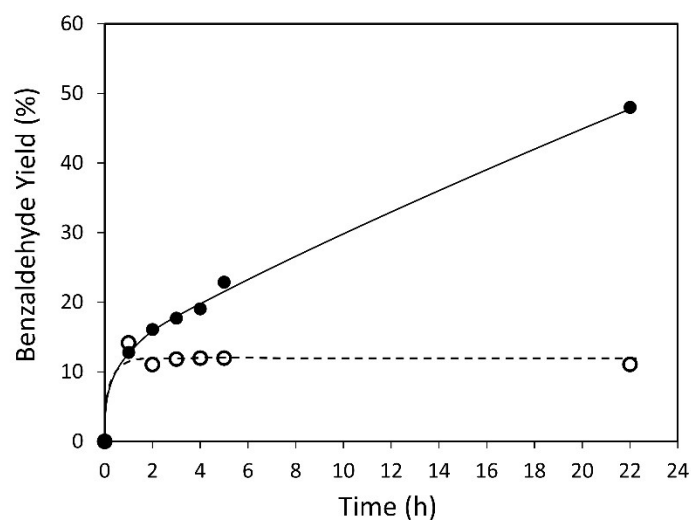


**Figure S7.** Hot catalyst filtration test: the catalyst (UiO-2-6) was removed by filtration from the reaction medium after 1 h of reaction (dashed line). The same reaction without removal of the catalyst is also shown (full line).

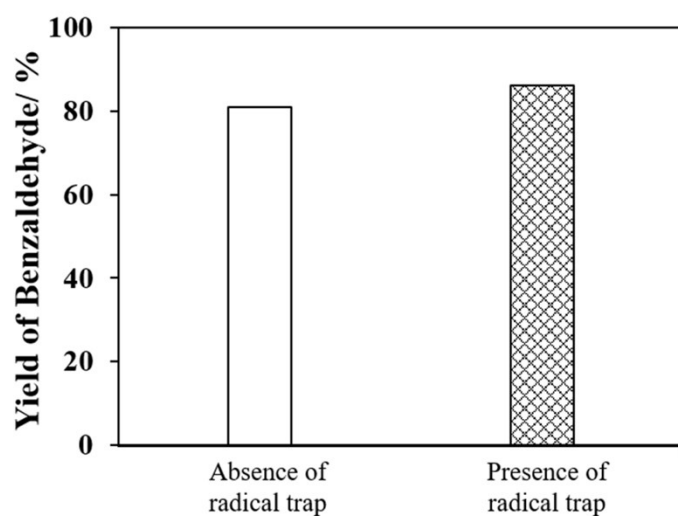


**Figure S8.** Effect of the addition of butylated hydroxytoluene, a common radical trap, upon the benzaldehyde yields. The experimental procedure followed for the catalytic test in the presence of the radical trap (dibutylated hydroxytoluene) was the same than that described in the experimental section of the same text. The two tests were achieved with the material UiO-2-9.

Test conditions: molar BA/TBHP ratio = 0.5,  $V_{\text{CH}_3\text{CN}} = 0.5$  mL,  $T = 40$  °C, time of reaction = 24 h.

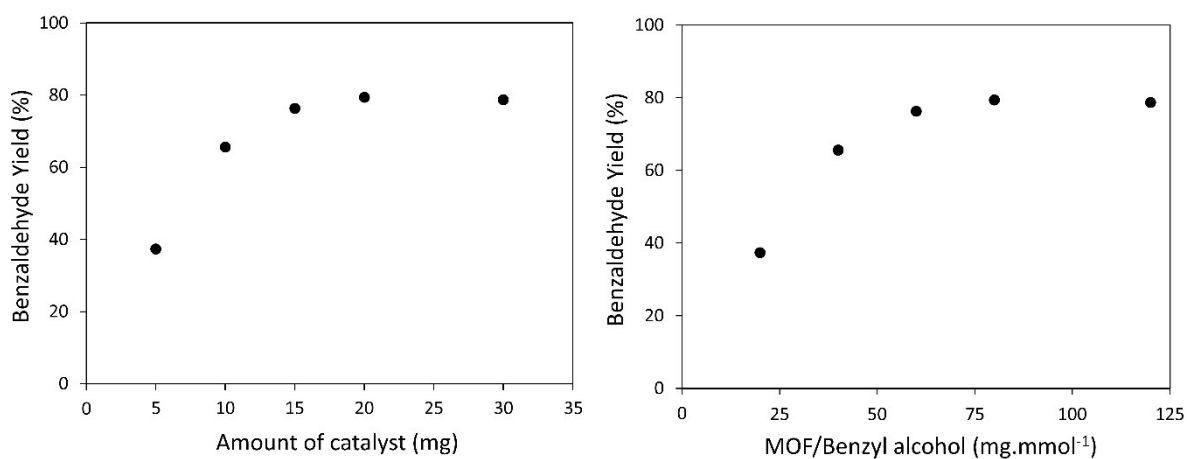


**Figure S9.** Effect of the amount of catalyst (UiO-1-9) over the benzaldehyde yield: the weight of catalyst introduced in the reaction mixture (left) and the weight of catalyst per mmol of benzyl alcohol (right).

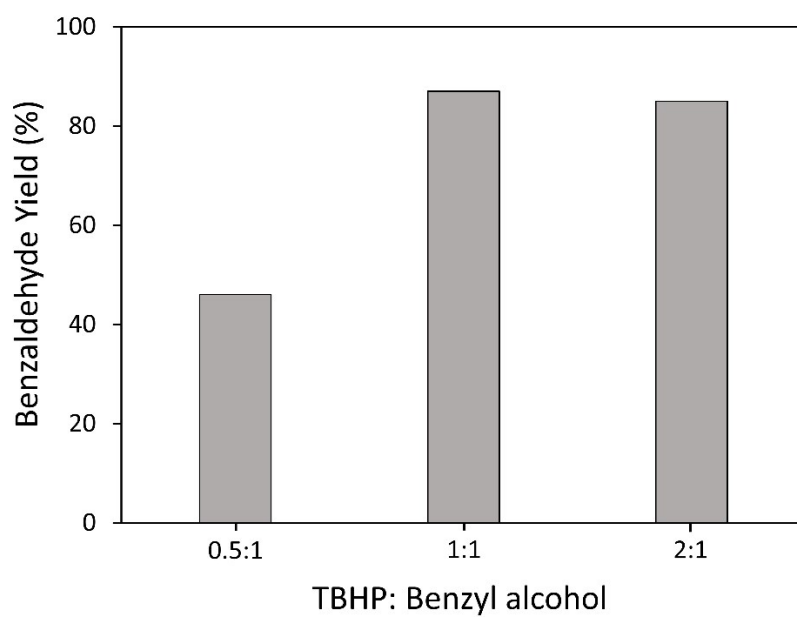


**Figure S10.** Effect of the molar ratio “TBHP/benzyl alcohol” over the benzaldehyde yield.

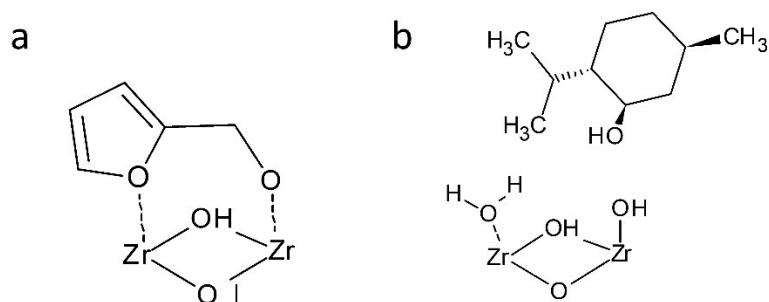


**Figure S11.** Proposed views of (a) furfuryl alcohol and (b) menthol interacting with the defective Zr-O(H)-Zr site of UiO-66. It is assumed that the coordination of the two adjacent Zr<sub>UC</sub> sites by the two oxygens of the furfuryl alcohol prevents the simultaneous coordination of the furfuryl alcohol and TBHP required for the alcohol dehydrogenation to proceed. It is also assumed that the bulky isopropyl moieties and 3-dimensional chemical structure of the cyclohexane ring of menthol prevent its coordination to the Zr<sub>UC</sub>.

## References.

- [1] L. Valenzano, B. Civalieri, S. Chavan, S. Bordiga, M. H. Nilsen, S. Jakobsen, K. P Lillerud, C. Lamberti, *Chem. Mater.*, 2011, **23**, 1700–1718.
- [2] L. Asgharnejad, A. Abbasi, M. Najafi, J. Janczak, *J. Solid State Chem.* 2019, **277**, 187–194.
- [3] A. Paul, L. M.D.R.S. Martins, A. Karmakar, M. L. Kuznetsov, A. S. Novikov, M. F. C. Guedes da Silva, A. J.L. Pombeiro, *J. Catal.*, 2020, **385**, 324–337.
- [4] S. Aryanejad, G. Bagherzade, A. Farrokhi *Appl Organometal Chem.* 2018; 32:e3995. <https://doi.org/10.1002/aoc.3995>
- [5] W. Jumpathong, T. Pila, Y. Lekjing, P. Chirawatkul, B. Boekfa, S. Horike, K. Kongpatpanich *APL Mater.* 2019, **7**, 111109.
- [6] N. A. Dare, L. Brammer, S. A. Bourn, T. J. Egan, *Inorg. Chem.* 2018, **57**, 3, 1171–1183.
- [7] A. Fidalgo-Marijuan, E. Amayuelas, G. Barandika, E. S. Larrea, B. Bazán, M. Karmele Urtiaga, M. Iglesias, M. I. Arriortua, *IUCrJ*, 2018, **5**, 59-568.
- [8] M. Saikia, D. Bhuyan, L. Saikia, *New J. Chem.* 2015, **39**, 64–67.
- [9] H. Liu, Y. Liu, Y. Li, Z. Tang, H. Jiang *J. Phys. Chem. C* 2010, **114**, 13362–13369.
- [10] T. Ishida, M. Nagaoka, T. Akita, M. Haruta *Chem. Eur. J.* 2008, **14**, 8456 – 8460.
- [11] J. Zhu, P. C. Wang, M. Lu *Applied Catalysis A: General* 2014, **477**, 125–131.
- [12] A. Dhakshinamoorthy, M. Alvaro, H. Garcia *ACS Catal.* 2011, **1**, 48–53.